Title

Associations among amyloid status, age, and longitudinal regional brain atrophy in cognitively unimpaired older adults

Authors

Nosheny, Rachel L
Insel, Philip S
Mattsson, Niklas
et al.

Publication Date

2019-10-01

DOI

10.1016/j.neurobiolaging.2019.07.005

Peer reviewed

HHS Public Access

Author manuscript

Neurobiol Aging. Author manuscript; available in PMC 2020 October 01.

Published in final edited form as:

Neurobiol Aging. 2019 October ; 82: 110–119. doi:10.1016/j.neurobiolaging.2019.07.005.

Associations among amyloid status, age, and longitudinal regional brain atrophy in cognitively unimpaired older adults

Rachel L. Nosheny[a,b,*], **Philip S. Insel**[c], **Niklas Mattsson**[c], **Duygu Tosun**[a,d], **Shannon Buckley**[a], **Diana Truran**[a], **N. Schuff**[a], **Paul S. Aisen**[e], **Michael W. Weiner**[a,b,d], **Alzheimer's Disease Neuroimaging Initiative**[1]

[a]Department of Veterans Affairs Medical Center, Center for Imaging of Neurodegenerative Diseases, San Francisco, CA, USA

[b]Department of Psychiatry, University of California, CA, USA

[c]Department of Clinical Sciences Malmö, Clinical Memory Research Unit, Lund University, Lund, Sweden

[d]Department of Radiology and Biomedical Imaging, University of California, CA, USA

[e]Alzheimer's Therapeutic Research Institute, Keck School of Medicine of USC, San Diego, CA, USA

Abstract

The goal of this study was to compare regional brain atrophy patterns in cognitively unimpaired (CU) older adults with and without brain accumulation of Amyloid-β (Aβ) to elucidate contributions of Aβ, age, and other variables to atrophy rates. In 80 CU participants from the Alzheimer's Disease Neuroimaging Initiative, we determined effects of Aβ and age on longitudinal, regional atrophy rates, while accounting for confounding variables including sex, *APOE* ε4 genotype, white matter lesions, and cerebrospinal fluid total and phosphorylated tau levels. We not only found overlapping patterns of atrophy in Aβ+ versus Aβ− participants but also

*Corresponding author at: Department of Veterans Affairs Medical Center, Center for Imaging of Neurodegenerative Diseases, 4150 Clement Street, 114M, San Francisco, CA, USA. Tel.: +1-650 468-0619; fax: + 1-415-668-2864. rachel.nosheny@ucsf.edu (R.L. Nosheny).

[1]Data used in preparation of this article were obtained from the Alzheimer's Disease Neuroimaging Initiative (ADNI) database (adni.loni.usc.edu). As such, the investigators within the ADNI contributed to the design and implementation of ADNI and/or provided data but did not participate in analysis or writing of this report. A complete listing of ADNI investigators can be found at: http://adni.loni.usc.edu/wp-content/uploads/how_to_apply/ADNI_Acknowledgement_List.pdf.

Disclosure

N.R.L., I.P.S., M.N., To.D., B.S., Tr.D., and S.N. have nothing to disclose. A.P.S. performed the following activities during the period of work, all outside of the scope of the submitted work, received personal fees from NeuroPhage; Elan Corporation; Wyeth; Eisai Inc; Schering-Plough Corp.; Bristol-Myers Squibb; Eli Lilly and Company; NeuroPhage; Merck & Co; Roche; Amgen; Genentech, Inc; Abbott; Pfizer Inc; Novartis; Bayer; Astellas; Dainippon; BioMarin; Solvay; Otsuka; Daiichi; AstraZeneca; Janssen; Medivation, Inc; Ichor; Toyama; Lundbeck; Biogen Idec; iPierian; Probiodrug; Somaxon; Biotie; Anavex; and Kyowa Hakko Kirin Pharma, and received grants from Lilly, Baxter, and FNIH. W.M.W. performed the following activities during the period of work, all outside of the scope of the submitted work, received personal fees from Pfizer; Janssen; KLJ Associates; Easton Associates; Harvard University; inThought Research; INC Research, Inc; University of California, Los Angeles (UCLA); Alzheimer's Drug Discovery Foundation (ADDF); Sanofi-Aventis Groupe; Avid RadioPharmaceuticals; Eli Lilly & Co, Paul Sabatier University; Novartis; Tohoku University; MCI Group, France; Travel eDreams, Inc, Neuroscience School of Advanced Studies (NSAS); Danone Trading, BV; CTAD ANT Congres; ADRC; and received grants/contracts from Merck, Avid RadioPharmaceuticals, and Janssen Pharmaceutical.

Appendix A. Supplementary data

Supplementary data to this article can be found online at https://doi.org/10.1016/j.neurobiolaging.2019.07.005.

identified regions where atrophy pattern differed between the 2 groups. Higher Aβ load was associated with increased longitudinal atrophy in the entorhinal cortex, amygdala, and hippocampus, even when accounting for age and other variables. Age was associated with atrophy in insula, fusiform gyrus, and isthmus cingulate, even when accounting for Aβ. We found age by Aβ interactions in the postcentral gyrus and lateral orbitofrontal cortex. These results elucidate the separate and related effects of age, Aβ, and other important variables on longitudinal brain atrophy rates in CU older adults.

Keywords

Amyloid-β; Aging; Brain atrophy; Alzheimer's disease

1. Introduction

Alzheimer's disease (AD) is characterized by plaques of Amyloid-β (Aβ) peptides, tangles of phosphorylated tau (pTau) proteins, and neurodegeneration with specific regional distributions. Aβ pathology is believed to begin to accumulate in the neocortex outside the temporal lobe, while tau pathology and neurodegeneration start in the temporal lobe, especially in the entorhinal cortex and hippocampus (Braak and Braak, 1995; Cardenas et al., 2003; Du et al., 2003; Glenner and Wong, 1984; Jack et al., 2010, 2013; Kosik et al., 1986; Palmqvist et al., 2017; Thal et al., 2002). AD pathology is accompanied by progressive memory dysfunction leading to a continuum of mild cognitive impairment (MCI) and finally dementia (Grundman et al., 2004; Morris et al., 2001; Petersen et al., 1999).

Both aging in older adults and AD are associated with brain atrophy. Brain changes with age occur throughout the lifespan. The results of the present study focus on changes in older adults. The extent to which the regional pattern of atrophy differs between aging and AD has been previously studied with inconsistent results (Fjell et al., 2014a). Past studies have shown that in older adults, age is associated with widespread regional brain volume reductions (Walhovd et al., 2005), with more prominent effects in prefrontal, parietal, and sensorimotor regions than temporal and occipital regions (Allen et al., 2005; Resnick et al., 2003). MCI and AD are associated with accelerated atrophy in the medial temporal lobe, temporoparietal, and medial parietal regions (Dickerson et al., 2009). Some recent studies suggest similar patterns of atrophy in normal aging and AD (Fjell et al., 2014b; Oh et al., 2013), whereas others identify differential patterns with some overlapping regions (Bakkour et al., 2013). The identification of different spatial and temporal patterns of atrophy between aging and AD is likely confounded by many factors. There are methodological inconsistencies, and heterogeneous atrophy patterns are associated with different rates of disease progression and biomarker profiles (Dong et al., 2016; Jack et al., 2017). Recent studies have also highlighted the interacting contributions of multiple factors to brain atrophy, including genetic risk factors, tau, and cerebrovascular factors (Crary et al., 2014; Fletcher et al., 2016; Josephs et al., 2017; Knopman et al., 2015; Mormino, 2014; Mormino et al., 2016; Wilson et al., 2013).

Identification of differential regional atrophy in aging and AD is further complicated by the fact that 20%–40% of older adult cognitively unimpaired (CU) participants have substantial Aβ deposition (Arriagada et al., 1992; Dickerson et al., 2011; Morris et al., 2009; Rowe et al., 2010). Fibrillar Aβ deposition, which can be directly assessed in vivo by positron emission tomography (PET) using the radiotracers Pittsburgh Compound B or (18)Florbetapir (AV45) (Clark et al., 2011; Jack et al., 2008b; Rowe et al., 2007), or reduced cerebrospinal fluid (CSF) Aβ levels, is associated with brain atrophy in CU participants (Becker et al., 2011; Fagan et al., 2009; Fjell et al., 2010a; Mormino et al., 2009; Schott et al., 2010; Storandt et al., 2009; Tosun et al., 2010). Previous cross-sectional studies have yielded conflicting results regarding associations between regional atrophy and Aβ in CU older adults, including whether or not differences in regional volumes can discriminate Aβ+ and Aβ− CU older adults (Whitwell et al., 2013). Some studies have found decreased hippocampal volume associated with Aβ (Bourgeat et al., 2010; Mormino et al., 2009; Storandt et al., 2009), whereas others have not (Chetelat et al., 2010). Previous studies have also reported decreased cortical thickness and gray matter volume in temporal (Bakkour et al., 2013; Dickerson et al., 2011; Oh et al., 2013), frontal (Becker et al., 2011; Dickerson et al., 2011; Oh et al., 2013), parietal (Becker et al., 2011; Oh et al., 2013), and cingulate cortices (Fjell et al., 2010b; Oh et al., 2013), as well as precuneus (Oh et al., 2013). Interestingly, a few studies also found high brain Aβ levels to be associated with increased brain volume in older adult CU participants (Chetelat et al., 2010; Johnson et al., 2014).

Recent longitudinal studies have consistently found associations between Aβ and brain atrophy, with variability in the regions of atrophy identified, for example: significant increase in atrophy rate in Aβ and correlation between baseline Aβ and atrophy rate, especially in the temporal neocortex and the posterior cingulate cortex (Chetelat et al., 2012); greater atrophy rate in the entorhinal cortex associated with Aβ positivity but only in pTau-positive participants (Desikan et al., 2011); Aβ positivity associated with greater atrophy rate in the temporal lobe (Dore et al., 2013; Fletcher et al., 2018; Nosheny et al., 2015), insula and posterior cingulate (Dore et al., 2013; Fletcher et al., 2018; Nosheny et al., 2015), or thalamus (Fletcher et al., 2018); volumetric reductions over one year in multiple brain areas regardless of AD risk factors (Fjell et al., 2013); and increased frontoparietal atrophy rates associated with emerging Aβ pathology (Mattsson et al., 2014). Elucidating the contribution of Aβ to atrophy has important implications for the design of future studies of variables that are associated with brain atrophy, as well as clinical trials of AD therapeutics in which Aβ reduction and brain atrophy are outcome measures.

The goal of this study was to compare the pattern of brain atrophy in Aβ+ and Aβ− CU older adults, taking into account the contributions of age and other important variables. The novelty of our work compared to past studies is (1) our results include analysis of longitudinal atrophy over 4 years with multiple data points; (2) our multivariable analyses account for important covariates that have previously been found to have independent associations with brain atrophy (Crivello et al., 2010) (Schott et al., 2010) (Carmichael et al., 2010; Constans et al., 1995; Cowell et al., 1994; Farias et al., 2012; Jagust et al., 2008; Sowell et al., 2007); (3) We considered interactions between Aβ and age when determining their contributions to regional atrophy. We tested the a priori hypothesis that Aβ-driven brain atrophy is an accelerated version of atrophy associated with aging, affecting the same

regions, but with an increased rate of atrophy. As an exploratory aspect of the study, we determined whether additional variables including sex, APOE ε4 genotype, white matter lesions (WMLs), CSF total tau and pTau, and intracranial volume (ICV) are significantly associated with regional brain atrophy in this population, and if so, which variables are associated with atrophy in which regions.

2. Methods

2.1. Participants

Data used in the preparation of this article were obtained from the Alzheimer's Disease Neuroimaging Initiative (ADNI) database (adni.loni.usc.edu). The ADNI was launched in 2003 as a public-private partnership, led by Principal Investigator Michael W. Weiner, MD. The primary goal of ADNI has been to test whether serial magnetic resonance imaging (MRI), PET, other biological markers, and clinical and neuropsychological assessment can be combined to measure the progression of MCI and early AD. For upto-date information, see www.adni-info.org.

All ADNI data were downloaded from the ADNI database (www.loni.ucla.edu/ADNI). We included CU ADNI participants with successful longitudinal FreeSurfer processing of MRI images (average number of images per participant = 4.6, minimum number of images per participant = 2, maximum number of images per participant = 6), as well as a valid test result for AV45 imaging. Participants were aged 55–91 years at baseline, English or Spanish speaking, and had an available study partner. All participants met ADNI inclusion criteria for CU at their baseline visit: Mini–Mental State Examination scores of 24–30 (Folstein et al., 1975), Clinical Dementia Rating of 0 and memory box score of 0 (Morris, 1993); absence of major depressive disorder, memory dysfunction (Wechsler, 1987), impairment in activities of daily living, MCI, or dementia; no memory complaints aside from those common to other normal subjects of that age range. Further details regarding ADNI inclusion and exclusion criteria can be found at http://adni.loni.usc.edu/methods/documents/. All ADNI data were downloaded from the ADNI database (www.loni.ucla.edu/ADNI). The demographics of participants included in this study are shown in Table 1.

2.2. T1-weighted magnetic resonance imaging

Participants underwent a standardized 1.5 or 3 Tesla MRI protocol (http://www.loni.ucla.edu/ADNI/Research/Cores/index.shtml) that was previously validated across sites by individualized protocols for each scanner (Jack et al., 2008a), adni.loni.ucla.edu/methods/documents/mri-protocols/. The ADNI MRI quality control center at the Mayo Clinic selected the MP-RAGE image with higher quality and corrected for system-specific image artifacts, as described in the study by Jack et al., 2008a.

2.3. FreeSurfer longitudinal processing

Automated volume measures from all regions of interest were downloaded from the ADNI LONI website. Automated volume measures were performed by ADNI staff with FreeSurfer software package, version 5.1. Volume measurements for each of 41 Free-Surfer regions shown in Table 2 were calculated by averaging the volume measurement at each time point

from the right and left sides of the region of interest. To reduce confounding effects of intraparticipant morphological variability, each participant's data series was processed by FreeSurfer longitudinal workflow (Fischl et al., 2002, 2004); see http://surfer.nmr.mgh.harvard.edu/fswiki/LongitudinalProcessing. Details of quality control procedures are at http://www.loni.ucla.edu/twiki/pub/ADNI/ADNIPostProc/UCSFFreeSurferMethodsSummary.pdf."

2.4. PET imaging

18F-AV45 (Florbetapir) mages were collected at multiple sites. Participants were injected with 10 mCi AV45, 4 dynamic acquisition frames were obtained 50–70 minutes after injection and coregistered to one another, averaged, interpolated to a uniform image and voxel size (160 × 106 × 96, 1.5 mm^3), and smoothed to a uniform resolution (8 mm FWHM). See also adni.loni.ucla.edu/about-data-samples/image-data. A mean cortical standardized uptake value ratio (SUVr) measure was derived by normalizing average retention values of cortical regions (anterior cingulate, frontal, lateral temporal, parietal cortex, and precuneus), to retention value of the whole cerebellum. We used previously established thresholds for florbetapir-PET (SUVr >1.11) to identify the presence of Aβ pathology (Joshi et al., 2012; Landau et al., 2012).

2.5. Statistical analysis

Baseline values of demographic variables were compared using the Wilcoxon-Mann-Whitney test and Fisher's exact test. Volume was regressed on time since initial scan (baseline time) using linear mixed effect (LME) models, with both a random intercept and slope to estimate individual regional atrophy rates, assuming a compound symmetry correlation structure. The LME model included Aβ (either AV45 SUVr as a continuous variable, or Aβ status, as indicated in Section 3), baseline time, and the interaction of Aβ and baseline time. For results, Section 3.2, an interaction between Aβ status and pTau was also considered. For multivariable models, *APOE* ε4 genotype, gender, education, WML, ICV, CSF total, and pTau were included in the model. APOE ε4 genotype was dichotomized as positive (having at least one APOE ε4 allele) or negative. Each predictor was evaluated both separately and in a full model, adjusting for all other predictors. To test the ability of the multivariable models to reduce residual error, R^2 values were compared after adding groups of predictive variables in a forward, stepwise set of models. For the analyses described in Section 3.4, we also considered an interaction between Aβ and age in the multivariable model.

For the analysis of effect size in Aβ+ and Aβ− participants (Table 2), volume was regressed on time since initial scan, separately in the Aβ+ and Aβ− subgroups. Effect sizes were calculated as the estimate β divided by the standard deviation (SD) of the effect. The SD used to calculate effect size was a function of the slope and the error variance components and follow-up time:

$$f_x = \frac{\beta}{\sqrt{\frac{\sigma_s + \sigma_e}{\sum (t - t_\mu)^2}}}$$

Where fx = effect size, β = effect estimate, σ_s slope variance, σ_e = error variance, t time = in years, and t_μ = mean time in years. Model fits were inspected by an analysis of the residuals. All statistics were performed using R (v. 2.8.1, The R Foundation for Statistical Computing).

Although we examined many brain regions, we report nominal p-values, without adjustment for multiple testing. We do so because the clear functional and anatomical relationships among the regions examined permit coherent sets of findings to reinforce each other rather than detract from one another. For example, for the examination of the associations between Aβ status and regional atrophy rate, the significant association found between multiple temporal lobe structures is supported by the functional and biological relatedness of the regions. Multiple comparison adjustment would require that each result detract from the others. We therefore rely on scientific judgment rather than formal adjustment methods to indicate where caution is warranted despite findings with $p < 0.05$. We also report both nominal and adjusted p-values in the Supplemental Materials (Table S1).

3. Results

3.1. Associations between Aβ and atrophy rate

We classified participants as Aβ+ or Aβ− and calculated atrophy rates for 41 FreeSurfer regions in each subgroup (Table 2). Using LME models, we identified 3 regions in which atrophy rate was significantly higher in Aβ+ versus Aβ−: the hippocampus, entorhinal cortex, and amygdala (Fig. 1). Using AV45 as a continuous measure rather than classifying participants as Aβ+ or Aβ− gave similar results (Supplemental Fig. 1).

We also measured the association between Aβ status and atrophy rate in models accounting for multiple confounding variables that have independent associations with regional atrophy rate: age, ApoE ε4 genotype, ICV, WMLs, and gender. The association between positive Aβ status and higher atrophy rate remained significant when accounting for confounding variables. Including WMLs in the model resulted in a significant ($p = 0.04$) association between Aβ+ and higher frontal pole atrophy rate. In the multivariable model, no significant associations between regional atrophy rates and variables other than Aβ or age were found for the regions shown in Fig. 1. However, a number of independent associations between these additional variables and regional atrophy rates were found in a series of univariable models (Supplemental Tables S2–S6).

3.2. Contributions of tau

pTau was significantly associated with atrophy rates in several regions in univariable models (Supplemental Table S6). When we included pTau in the multivariable model, the areas with significant associations between Aβ+ and higher atrophy rate were the amygdala ($p = 0.04$) and entorhinal cortex ($p = 0.0014$). In this model including pTau, there was no significant association between Aβ and hippocampal atrophy ($p = 0.07$). We also considered Aβ by pTau interactions in a separate series of multivariable models. We found significant interactions between Aβ and pTau in their associations with atrophy in the fusiform gyrus ($p = 0.008$); the association between Aβ and atrophy rate was significantly higher in those with higher pTau levels.

3.3. Regions showing a significant association between age and longitudinal atrophy rate

LME models were used to determine the relationship between age and regional atrophy rate. In a univariable model including only age as the independent variable, significant associations were found between advanced age and higher atrophy rate in the lingual gyrus ($p = 0.03$) and temporal pole ($p = 0.01$). However, when accounting for the effects of Aβ status and age together in a multivariable model, we found significant associations between advanced age and higher atrophy rate in the insula ($p = 0.05$), fusiform gyrus ($p = 0.03$), and isthmus cingulate ($p = 0.05$) (Fig. 2). The associations retained significance in multivariable models including the covariates described previously. Fig. 3 summarizes the anatomical relationships between regions in which there are significant associations between higher atrophy rate and advanced age in univariable and multivariable models.

3.4. Regions with differential age-related atrophy rate in Aβ+ and Aβ− participants

To determine which regions have different age-related atrophy in Aβ+ and Aβ− participants, we considered an interaction between age and Aβ status in their association with atrophy rate. We identified 2 regions with significant interactions: postcentral gyrus (β = −19.00, SE = 6.80, $p = 0.006$), and lateral orbitofrontal cortex (β = 8.12, SE = 4.19, $p = 0.05$). In the postcentral gyrus, age-related atrophy was greater in Aβ+ than in Aβ− participants (Fig. 4A). Conversely, in the lateral orbitofrontal cortex, age-related atrophy was greater in Aβ− participants than in Aβ+ participants (Fig. 4B).

4. Discussion

The major findings of this study are the following: (1) in CU older adults, higher 4-year atrophy rates in several temporal lobe regions are significantly associated with Aβ+ status, with the strongest associations in the entorhinal cortex and amygdala (Section 3.1); (2) significant associations between Aβ status and higher atrophy rates in these regions exist even after accounting for several covariates, such as APOE ε4 genotype, gender, WMLs (a marker of cerebrovascular disease), and ICV (Section 3.1); (3) advanced age is significantly associated with higher atrophy rates in the insula, fusiform gyrus, and isthmus cingulate, even when accounting for Aβ (Section 3.3); and (4) 2 regions show an interaction between Aβ status and age in the association with atrophy rate. In the postcentral gyrus, there was accelerated age-related atrophy in Aβ+ participants, and in the lateral orbitofrontal cortex, there was accelerated age-related atrophy in Aβ− participants (Section 3.4).

We found significant associations between Aβ+ and brain atrophy in the entorhinal cortex, hippocampus, and amygdala. Using multivariable models, we demonstrated that the effect is unlikely to be confounded by other variables that have independent association with atrophy rate in some regions, including some related to other types of neurodegeneration (Section 3.1 and Tables S1–S6). Many of the previous cross-sectional and longitudinal work measuring associations between brain atrophy and Aβ specifically analyzed changes in the temporal lobe (Becker et al., 2011; Bourgeat et al., 2010; Desikan et al., 2011; Mormino et al., 2009; Nosheny et al., 2015) or focused on cortical thinning (Becker et al., 2011; Dickerson et al., 2009, 2011; Dore et al., 2013). In contrast, we measured associations between Aβ and atrophy rates in multiple regions. This informs us about associations

between individual regional atrophy rates and Aβ status but fails to answer the question of whether there are differences in the overall spatial pattern of atrophy across multiple brain regions. Therefore, we also compared effect sizes in the 2 groups (Table 2) to give a more global picture of atrophy pattern. Comparing atrophy rates by effect size separately in Aβ+ and Aβ− participants demon strated that in both groups, highest rates of brain atrophy are in temporal lobe regions including the hippocampus, parahippocampus, entorhinal cortex, and the superior, middle, and inferior temporal cortices (Table 2).

Our results on the association between regional brain atrophy and Aβ are consistent with some recent longitudinal studies (Fjell et al., 2009, 2014a; Mattsson et al., 2014). Like Chetelat et al., 2012 and Fletcher et al., 2018, we found accelerated atrophy associated with Aβ in the temporal lobe. Unlike Chetelat et al., 2012, we did not find accelerated atrophy in the cingulate cortex, superior and middle frontal gyri, temporo-occipital regions, medial temporal lobe, or precuneus. Unlike Fletcher et al., 2018, we did not find associations between Aβ and atrophy in the parahippocampal gyrus, thalamus, or parieto-temporal regions. The discrepancies may be explained by different cohorts and different methodology. For example, Fletcher et al., 2018 used CSF Aβ as a continuous measure. One important note is that the previous important articles analyzing longitudinal atrophy did so over a period of two years or less. In contrast, our data include analysis of longitudinal atrophy over four years with multiple data points. The longer period of observation time in our analysis allows for greater sensitivity to detect small changes and to detect differences between regions. Furthermore, in contrast, our data analyze atrophy in the entire brain using all the regions parcellated by FreeSurfer. Therefore, our results measuring regional atrophy throughout the brain, across a longer time span with multiple data points, and accounting for important covariates that have previously been found to have independent associations with brain atrophy, are new and add to previous reported findings.

Interestingly, atrophy rates in the entorhinal cortex and amygdala were most strongly associated with Aβ status. The association between Aβ status and hippocampal atrophy rate is weaker and loses significance when accounting for pTau. This is in line with the finding of a significant association between Aβ and longitudinal entorhinal atrophy only in CU participants classified as pTau positive (Desikan et al., 2011). Unlike previous cross-sectional studies (Bakkour et al., 2013; Becker et al., 2011; Bourgeat et al., 2010; Chetelat et al., 2010; Dickerson et al., 2011; Fjell et al., 2010b; Mormino et al., 2009; Oh et al., 2013; Storandt et al., 2009), we did not find areas outside of the temporal lobe with a significant association between Aβ status and atrophy rate. Thus, although Aβ status may be associated with baseline volume in many different regions, we find that Aβ status is only associated with longitudinal atrophy rates in the temporal lobe, with the strongest associations in the entorhinal cortex and amygdala.

In CU older adults, age was significantly associated with atrophy in different brain regions depending on whether or not Aβ was accounted for in the model. In a univariable model using age alone, there was a significant association between age and atrophy rate in the lingual gyrus and temporal pole. When we included Aβ status in the model, we found a significant association between age and atrophy rate in the insula, fusiform gyrus, and isthmus cingulate. There are 2 main conclusions from the age data. First, age-related atrophy

involves multiple medial temporal lobe brain regions. Although the regions independently associated with age are adjacent to the regions independently associated with Aβ, there is no overlap in regions. This finding contrasts those of cross-sectional studies in which age was found to be associated with widespread reductions in volume and cortical thickness, independent of Aβ status (Becker et al., 2011; Oh et al., 2013). Thus, the interdependence of age and Aβ in determining brain atrophy differs when using baseline volume versus longitudinal atrophy rate as an outcome measure. Furthermore, regional atrophy associated with age depends on Aβ status in this cohort, and it is therefore crucial to account for Aβ in models of age effects on regional atrophy. It is important to point out that our results focus solely on the effects of aging in older adults and therefore cannot address effects of age observed across the lifespan.

Although age, independent of Aβ, is associated with atrophy in different brain regions, this effect is likely mediated by a combination of the effects of “normal aging” together with other factors responsible for neurodegeneration, including tau, cerebrovascular factors, genetic risk factors, and inflammation (Deming et al., 2017; Irwin et al., 2017; Josephs et al., 2017; Mormino et al., 2016; Wilson et al., 2013). Although this work does not address the contribution of each of these pathologies to regional atrophy, we do address contributions of CSF pTau and WML in addition to Aβ.

To identify regions in which age-related atrophy differs in Aβ+ versus Aβ− participants, we tested for an interaction between age and Aβ status in our models and identified only 2 regions with a significant interaction. In the postcentral gyrus, age-related atrophy rate is greater in Aβ+ participants than in Aβ− participants. Conversely, in the lateral orbitofrontal cortex, age-related atrophy is greater in Aβ− participants than in Aβ+. The significance of this novel finding is not entirely clear. Others have previously found increased gray matter and hypermetabolism associated with high levels of brain Aβ in temporal and parietal regions in CU (Chetelat et al., 2010; Fortea et al., 2011; Iacono et al., 2008; Johnson et al., 2014) Aβ+ participants. Some of these studies suggest that such changes may be due to inflammation or compensation for atrophy or that they may be driven by a subset of Aβ+CU individuals who are resistant to the neurodegenerative and/or cognitive effects of Aβ due to some unknown protective factor. Further investigation of cognitive status in this cohort is necessary to investigate this possibility.

Although this study provides important new information about the factors contributing to regional brain atrophy in older adults, it has limitations. First, the ADNI cohort may not accurately reflect the population in terms of atrophy in CU participants (Whitwell et al., 2012), and ADNI exclusion criteria limit the range of values of variables such as WML, so that effects of WML may be underestimated in our model. Second, because we use a single Aβ measurement to classify participants as Aβ+ or Aβ−, we cannot fully account for the role of emerging Aβ pathology in our model (Mattsson et al., 2014). In addition, the vast majority of participants had AV45 PET performed after the final MRI used to calculate atrophy rate (see Section 2). Thus, our Aβ+ group includes both those who were Aβ+ at baseline and those who developed significant Aβ+ accumulation over the course of the study, including those who became Aβ+ after the volume measurements were made. To rule out the possibility that using a dichotomous Aβ measure obscured the role of emerging Aβ

pathology on brain atrophy, we confirmed these results using AV45 SUVr as a continuous measure (Supplemental Fig. 1). Furthermore, 58% of participants in this study also had CSF Aβ 1–42 measured at baseline, and of these, 93% had agreement between Aβ status measured using CSF Aβ 1–42 and AV45, suggesting that our Aβ+ cohort does not include many participants who were Aβ− at baseline. Another limitation is that we relied on CSF pTau and total tau measurements. Because the associations between CSF tau measures and tau accumulation measured by tau PET imaging is only modest (Mattsson et al., 2017) and CSF tau is an overall measure which does not give any information about local tau pathology, it would be interesting to complement the current analysis with regional tau PET data in future studies.

Although we examined many brain regions, we report nominal *p*-values, without adjustment for multiple testing, throughout the article. We do so because multiple comparison adjustment would require that each result detract from the others, but the clear functional and anatomical relationships among the regions examined permit coherent sets of findings to reinforce each other rather than detract from one another. However, we acknowledge that thresholding for a nominal *p*-vlaue of 0.05 when comparing a large number of brain regions of interest is permissive. Therefore, we report both nominal and adjusted *p*-values (see Supplemental Table S1), and we rely on scientific judgment rather than formal adjustment methods to indicate where caution is warranted despite findings with $p < 0.05$.

5. Conclusions

These findings elucidate the separate and related effects of age, Aβ, and other factors that may be associated with age on longitudinal brain atrophy rates in CU older adults. We identified the hippocampus, amygdala, and entorhinal cortex as specific brain regions in which Aβ is associated with atrophy when accounting for age; the insula, fusiform gyrus, and isthmus cingulate as specific regions where atrophy is associated with age, even when accounting for Aβ; and the postcentral gyrus and lateral orbitofrontal cortex as regions with differential age-related atrophy in Aβ+ and Aβ− CU older adults.

Supplementary Material

Refer to Web version on PubMed Central for supplementary material.

Acknowledgements

Data collection and sharing for this project was funded by the Alzheimer's Disease Neuroimaging Initiative (ADNI) (National Institutes of Health Grant U01 AG024904) and DOD ADNI (Department of Defense award number W81XWH-12-2-0012). ADNI is funded by the National Institute on Aging, the National Institute of Biomedical Imaging and Bioengineering, and through generous contributions from the following: AbbVie, Alzheimer's Association; Alzheimer's Drug Discovery Foundation; Araclon Biotech; Bio-Clinica, Inc; Biogen; Bristol-Myers Squibb Company; CereSpir, Inc; Cogstate; Eisai Inc; Elan Pharmaceuticals, Inc; Eli Lilly and Company; EuroImmun; F. Hoffmann-La Roche Ltd and its affiliated company Genentech, Inc; Fujirebio; GE Healthcare; IXICO Ltd; Janssen Alzheimer Immunotherapy Research & Development, LLC.; Johnson & Johnson Pharmaceutical Research & Development LLC.; Lumosity; Lundbeck; Merck & Co, Inc; Meso Scale Diagnostics, LLC.; NeuroRx Research; Neurotrack Technologies; Novartis Pharmaceuticals Corporation; Pfizer Inc; Piramal Imaging; Servier; Takeda Pharmaceutical Company; and Transition Therapeutics. The Canadian Institutes of Health Research is providing funds to support ADNI clinical sites in Canada. Private sector contributions are facilitated by the Foundation for the National Institutes of Health (www.fnih.org). The grantee organization is the Northern California Institute for Research and Education, and the study is coordinated by the Alzheimer's Therapeutic

Research Institute at the University of Southern California. ADNI data are disseminated by the Laboratory for Neuro Imaging at the University of Southern California.

References

Allen JS, Bruss J, Brown CK, Damasio H, 2005 Normal neuroanatomical variation due to age: the major lobes and a parcellation of the temporal region. Neurobiol. Aging 26, 1245–1260. [PubMed: 16046030]

Arriagada PV, Marzloff K, Hyman BT, 1992 Distribution of Alzheimer-type pathologic changes in nondemented elderly individuals matches the pattern in Alzheimer's disease. Neurology 42, 1681–1688. [PubMed: 1307688]

Bakkour A, Morris JC, Wolk DA, Dickerson BC, 2013 The effects of aging and Alzheimer's disease on cerebral cortical anatomy: specificity and differential relationships with cognition. Neuroimage 76, 332–344. [PubMed: 23507382]

Becker JA, Hedden T, Carmasin J, Maye J, Rentz DM, Putcha D, Fischl B, Greve DN, Marshall GA, Salloway S, Marks D, Buckner RL, Sperling RA, Johnson KA, 2011 Amyloid-beta associated cortical thinning in clinically normal elderly. Ann. Neurol 69, 1032–1042. [PubMed: 21437929]

Bourgeat P, Chetelat G, Villemagne VL, Fripp J, Raniga P, Pike K, Acosta O, Szoeke C, Ourselin S, Ames D, Ellis KA, Martins RN, Masters CL, Rowe CC, Salvado O, 2010 Beta-amyloid burden in the temporal neocortex is related to hippocampal atrophy in elderly subjects without dementia. Neurology 74, 121–127. [PubMed: 20065247]

Braak H, Braak E, 1995 Staging of Alzheimer's disease-related neurofibrillary changes. Neurobiol. Aging 16, 271–278. [PubMed: 7566337]

Cardenas VA, Du AT, Hardin D, Ezekiel F, Weber P, Jagust WJ, Chui HC, Schuff N, Weiner MW, 2003 Comparison of methods for measuring longitudinal brain change in cognitive impairment and dementia. Neurobiol. Aging 24, 537–544. [PubMed: 12714110]

Carmichael O, Schwarz C, Drucker D, Fletcher E, Harvey D, Beckett L, Jack CR Jr., Weiner M, DeCarli C, 2010 Longitudinal changes in white matter disease and cognition in the first year of the Alzheimer disease neuroimaging initiative. Arch. Neurol 67, 1370–1378. [PubMed: 21060014]

Chetelat G, Villemagne VL, Pike KE, Baron JC, Bourgeat P, Jones G, Faux NG, Ellis KA, Salvado O, Szoeke C, Martins RN, Ames D, Masters CL, Rowe CC, 2010 Larger temporal volume in elderly with high versus low beta-amyloid deposition. Brain 133, 3349–3358. [PubMed: 20739349]

Chetelat G, Villemagne VL, Villain N, Jones G, Ellis KA, Ames D, Martins RN, Masters CL, Rowe CC, Group AR, 2012 Accelerated cortical atrophy in cognitively normal elderly with high beta-amyloid deposition. Neurology 78, 477–484. [PubMed: 22302548]

Clark CM, Schneider JA, Bedell BJ, Beach TG, Bilker WB, Mintun MA, Pontecorvo MJ, Hefti F, Carpenter AP, Flitter ML, Krautkramer MJ, Kung HF, Coleman RE, Doraiswamy PM, Fleisher AS, Sabbagh MN, Sadowsky CH, Reiman EP, Zehntner SP, Skovronsky DM, 2011 Use of florbetapir-PET for imaging beta-amyloid pathology. JAMA 305, 275–283. [PubMed: 21245183]

Constans JM, Meyerhoff DJ, Gerson J, MacKay S, Norman D, Fein G, Weiner MW, 1995 H-1 MR spectroscopic imaging of white matter signal hyperintensities: alzheimer disease and ischemic vascular dementia. Radiology 197, 517–523. [PubMed: 7480705]

Cowell PE, Turetsky BI, Gur RC, Grossman RI, Shtasel DL, Gur RE, 1994 Sex differences in aging of the human frontal and temporal lobes. J. Neurosci 14, 4748–4755. [PubMed: 8046448]

Crary JF, Trojanowski JQ, Schneider JA, Abisambra JF, Abner EL, Alafuzoff I, Arnold SE, Attems J, Beach TG, Bigio EH, Cairns NJ, Dickson DW, Gearing M, Grinberg LT, Hof PR, Hyman BT, Jellinger K, Jicha GA, Kovacs GG, Knopman DS, Kofler J, Kukull WA, Mackenzie IR, Masliah E, McKee A, Montine TJ, Murray ME, Neltner JH, Santa-Maria I, Seeley WW, Serrano-Pozo A, Shelanski ML, Stein T, Takao M, Thal DR, Toledo JB, Troncoso JC, Vonsattel JP, White CL 3rd, Wisniewski T, Woltjer RL, Yamada M, Nelson PT, 2014 Primary age-related tauopathy (PART): a common pathology associated with human aging. Acta Neuropathol. 128, 755–766. [PubMed: 25348064]

Crivello F, Lemaitre H, Dufouil C, Grassiot B, Delcroix N, Tzourio-Mazoyer N, Tzourio C, Mazoyer B, 2010 Effects of ApoE-epsilon4 allele load and age on the rates of grey matter and hippocampal

volumes loss in a longitudinal cohort of 1186 healthy elderly persons. Neuroimage 53, 1064–1069. [PubMed: 20060049]

Deming Y, Li Z, Kapoor M, Harari O, Del-Aguila JL, Black K, Carrell D, Cai Y, Fernandez MV, Budde J, Ma S, Saef B, Howells B, Huang KL, Bertelsen S, Fagan AM, Holtzman DM, Morris JC, Kim S, Saykin AJ, De Jager PL, Albert M, Moghekar A, O'Brien R, Riemenschneider M, Petersen RC, Blennow K, Zetterberg H, Minthon L, Van Deerlin VM, Lee VM, Shaw LM, Trojanowski JQ, Schellenberg G, Haines JL, Mayeux R, Pericak-Vance MA, Farrer LA, Peskind ER, Li G, Di Narzo AF, Alzheimer's Disease Neuroimaging I, Alzheimer Disease Genetic C, Kauwe JS, Goate AM, Cruchaga C, 2017 Genome-wide association study identifies four novel loci associated with Alzheimer's endophenotypes and disease modifiers. Acta Neuropathol. 133, 839–856. [PubMed: 28247064]

Desikan RS, McEvoy LK, Thompson WK, Holland D, Roddey JC, Blennow K, Aisen PS, Brewer JB, Hyman BT, Dale AM, 2011 Amyloid-beta associated volume loss occurs only in the presence of phospho-tau. Ann. Neurol 70, 657–661. [PubMed: 22002658]

Dickerson BC, Bakkour A, Salat DH, Feczko E, Pacheco J, Greve DN, Grodstein F, Wright CI, Blacker D, Rosas HD, Sperling RA, Atri A, Growdon JH, Hyman BT, Morris JC, Fischl B, Buckner RL, 2009 The cortical signature of Alzheimer's disease: regionally specific cortical thinning relates to symptom severity in very mild to mild AD dementia and is detectable in asymptomatic amyloid-positive individuals. Cereb. Cortex 19, 497–510. [PubMed: 18632739]

Dickerson BC, Stoub TR, Shah RC, Sperling RA, Killiany RJ, Albert MS, Hyman BT, Blacker D, Detoledo-Morrell L, 2011 Alzheimer-signature MRI biomarker predicts AD dementia in cognitively normal adults. Neurology 76, 1395–1402. [PubMed: 21490323]

Dong A, Toledo JB, Honnorat N, Doshi J, Varol E, Sotiras A, Wolk D, Trojanowski JQ, Davatzikos C, Alzheimer's Disease Neuroimaging I, 2016 Heterogeneity of neuroanatomical patterns in prodromal Alzheimer's disease: links to cognition, progression and biomarkers. Brain 140, 735–747.

Dore V, Villemagne VL, Bourgeat P, Fripp J, Acosta O, Chetelat G, Zhou L, Martins R, Ellis KA, Masters CL, Ames D, Salvado O, Rowe CC, 2013 Cross-sectional and longitudinal analysis of the relationship between Abeta deposition, cortical thickness, and memory in cognitively unimpaired individuals and in Alzheimer disease. JAMA Neurol. 70, 903–911. [PubMed: 23712469]

Du AT, Schuff N, Zhu XP, Jagust WJ, Miller BL, Reed BR, Kramer JH, Mungas D, Yaffe K, Chui HC, Weiner MW, 2003 Atrophy rates of entorhinal cortex in AD and normal aging. Neurology 60, 481–486. [PubMed: 12578931]

Fagan AM, Head D, Shah AR, Marcus D, Mintun M, Morris JC, Holtzman DM, 2009 Decreased cerebrospinal fluid Abeta(42) correlates with brain atrophy in cognitively normal elderly. Ann. Neurol 65, 176–183. [PubMed: 19260027]

Farias ST, Mungas D, Reed B, Carmichael O, Beckett L, Harvey D, Olichney J, Simmons A, Decarli C, 2012 Maximal brain size remains an important predictor of cognition in old age, independent of current brain pathology. Neurobiol. Aging 33, 1758–1768. [PubMed: 21531482]

Fischl B, Salat DH, Busa E, Albert M, Dieterich M, Haselgrove C, van der Kouwe A, Killiany R, Kennedy D, Klaveness S, Montillo A, Makris N, Rosen B, Dale AM, 2002 Whole brain segmentation: automated labeling of neuroanatomical structures in the human brain. Neuron 33, 341–355. [PubMed: 11832223]

Fischl B, van der Kouwe A, Destrieux C, Halgren E, Segonne F, Salat DH, Busa E, Seidman LJ, Goldstein J, Kennedy D, Caviness V, Makris N, Rosen B, Dale AM, 2004 Automatically parcellating the human cerebral cortex. Cereb. Cortex 14, 11–22. [PubMed: 14654453]

Fjell AM, McEvoy L, Holland D, Dale AM, Walhovd KB, Alzheimer's Disease Neuroimaging I, 2013 Brain changes in older adults at very low risk for Alzheimer's disease. J. Neurosci 33, 8237–8242. [PubMed: 23658162]

Fjell AM, McEvoy L, Holland D, Dale AM, Walhovd KB, Alzheimer's Disease Neuroimaging I, 2014a What is normal in normal aging? Effects of aging, amyloid and Alzheimer's disease on the cerebral cortex and the hippocampus. Prog. Neurobiol 117, 20–40. [PubMed: 24548606]

Fjell AM, Walhovd KB, Fennema-Notestine C, McEvoy LK, Hagler DJ, Holland D, Blennow K, Brewer JB, Dale AM, 2010a Brain atrophy in healthy aging is related to CSF levels of Abeta1–42. Cereb. Cortex 20, 2069–2079. [PubMed: 20051356]

Fjell AM, Walhovd KB, Fennema-Notestine C, McEvoy LK, Hagler DJ, Holland D, Brewer JB, Dale AM, 2009 One-year brain atrophy evident in healthy aging. J. Neurosci 29, 15223–15231. [PubMed: 19955375]

Fjell AM, Walhovd KB, Fennema-Notestine C, McEvoy LK, Hagler DJ, Holland D, Brewer JB, Dale AM, 2010b CSF biomarkers in prediction of cerebral and clinical change in mild cognitive impairment and Alzheimer's disease. J. Neurosci 30, 2088–2101. [PubMed: 20147537]

Fjell AM, Westlye LT, Grydeland H, Amlien I, Espeseth T, Reinvang I, Raz N, Dale AM, Walhovd KB, Alzheimer Disease Neuroimaging I, 2014b Accelerating cortical thinning: unique to dementia or universal in aging? Cereb. Cortex 24, 919–934. [PubMed: 23236213]

Fletcher E, Filshtein TJ, Harvey D, Renaud A, Mungas D, DeCarli C, 2018 Staging of amyloid beta, t-tau, regional atrophy rates, and cognitive change in a nondemented cohort: results of serial mediation analyses. Alzheimers Dement. (Amst) 10, 382–393. [PubMed: 29984299]

Fletcher E, Villeneuve S, Maillard P, Harvey D, Reed B, Jagust W, DeCarli C, 2016 beta-amyloid, hippocampal atrophy and their relation to longitudinal brain change in cognitively normal individuals. Neurobiol. Aging 40, 173–180. [PubMed: 26973117]

Folstein MF, Folstein SE, McHugh PR, 1975 Mini-mental state". A practical method for grading the cognitive state of patients for the clinician. J. Psychiatr. Res 12, 189–198. [PubMed: 1202204]

Fortea J, Sala-Llonch R, Bartres-Faz D, Llado A, Sole-Padulles C, Bosch B, Antonell A, Olives J, Sanchez-Valle R, Molinuevo JL, Rami L, 2011 Cognitively preserved subjects with transitional cerebrospinal fluid ss-amyloid 1–42 values have thicker cortex in Alzheimer's disease vulnerable areas. Biol. Psychiatry 70, 183–190. [PubMed: 21514924]

Glenner GG, Wong CW, 1984 Alzheimer's disease: initial report of the purification and characterization of a novel cerebrovascular amyloid protein. Biochem. Biophys. Res. Commun 120, 885–890. [PubMed: 6375662]

Grundman M, Petersen RC, Ferris SH, Thomas RG, Aisen PS, Bennett DA, Foster NL, Jack CR Jr., Galasko DR, Doody R, Kaye J, Sano M, Mohs R, Gauthier S, Kim HT, Jin S, Schultz AN, Schafer K, Mulnard R, van Dyck CH, Mintzer J, Zamrini EY, Cahn-Weiner D, Thal LJ, 2004 Mild cognitive impairment can be distinguished from Alzheimer disease and normal aging for clinical trials. Arch. Neurol 61, 59–66. [PubMed: 14732621]

Iacono D, O'Brien R, Resnick SM, Zonderman AB, Pletnikova O, Rudow G, An Y, West MJ, Crain B, Troncoso JC, 2008 Neuronal hypertrophy in asymptomatic Alzheimer disease. J. Neuropathol. Exp. Neurol 67, 578–589. [PubMed: 18520776]

Irwin DJ, Grossman M, Weintraub D, Hurtig HI, Duda JE, Xie SX, Lee EB, Van Deerlin VM, Lopez OL, Kofler JK, Nelson PT, Jicha GA, Woltjer R, Quinn JF, Kaye J, Leverenz JB, Tsuang D, Longfellow K, Yearout D, Kukull W, Keene CD, Montine TJ, Zabetian CP, Trojanowski JQ, 2017 Neuropathological and genetic correlates of survival and dementia onset in synucleinopathies: a retrospective analysis. Lancet Neurol. 16, 55–65. [PubMed: 27979356]

Jack CR Jr., Bernstein MA, Fox NC, Thompson P, Alexander G, Harvey D, Borowski B, Britson PJ, L Whitwell J, Ward C, Dale AM, Felmlee JP, Gunter JL, Hill DL, Killiany R, Schuff N, Fox-Bosetti S, Lin C, Studholme C, DeCarli CS, Krueger G, Ward HA, Metzger GJ, Scott KT, Mallozzi R, Blezek D, Levy J, Debbins JP, Fleisher AS, Albert M, Green R, Bartzokis G, Glover G, Mugler J, Weiner MW, 2008a The alzheimer's disease neuroimaging initiative (ADNI): MRI methods. J. Magn. Reson. Imaging 27, 685–691. [PubMed: 18302232]

Jack CR Jr., Knopman DS, Jagust WJ, Petersen RC, Weiner MW, Aisen PS, Shaw LM, Vemuri P, Wiste HJ, Weigand SD, Lesnick TG, Pankratz VS, Donohue MC, Trojanowski JQ, 2013 Tracking pathophysiological processes in Alzheimer's disease: an updated hypothetical model of dynamic biomarkers. Lancet Neurol. 12, 207–216. [PubMed: 23332364]

Jack CR Jr., Knopman DS, Jagust WJ, Shaw LM, Aisen PS, Weiner MW, Petersen RC, Trojanowski JQ, 2010 Hypothetical model of dynamic biomarkers of the Alzheimer's pathological cascade. Lancet Neurol. 9, 119–128. [PubMed: 20083042]

Jack CR Jr., Lowe VJ, Senjem ML, Weigand SD, Kemp BJ, Shiung MM, Knopman DS, Boeve BF, Klunk WE, Mathis CA, Petersen RC, 2008b 11C PiB and structural MRI provide complementary information in imaging of Alzheimer's disease and amnestic mild cognitive impairment. Brain 131, 665–680. [PubMed: 18263627]

Jack CR Jr., Wiste HJ, Weigand SD, Therneau TM, Knopman DS, Lowe V, Vemuri P, Mielke MM, Roberts RO, Machulda MM, Senjem ML, Gunter JL, Rocca WA, Petersen RC, 2017 Age-specific and sex-specific prevalence of cerebral beta-amyloidosis, tauopathy, and neurodegeneration in cognitively unimpaired individuals aged 50–95 years: a cross-sectional study. Lancet Neurol. 16, 435–444. [PubMed: 28456479]

Jagust WJ, Zheng L, Harvey DJ, Mack WJ, Vinters HV, Weiner MW, Ellis WG, Zarow C, Mungas D, Reed BR, Kramer JH, Schuff N, DeCarli C, Chui HC, 2008 Neuropathological basis of magnetic resonance images in aging and dementia. Ann. Neurol 63, 72–80. [PubMed: 18157909]

Johnson SC, Christian BT, Okonkwo OC, Oh JM, Harding S, Xu G, Hillmer AT, Wooten DW, Murali D, Barnhart TE, Hall LT, Racine AM, Klunk WE, Mathis CA, Bendlin BB, Gallagher CL, Carlsson CM, Rowley HA, Hermann BP, Dowling NM, Asthana S, Sager MA, 2014 Amyloid burden and neural function in people at risk for Alzheimer's Disease. Neurobiol. Aging 35, 576–584. [PubMed: 24269021]

Josephs KA, Murray ME, Tosakulwong N, Whitwell JL, Knopman DS, Machulda MM, Weigand SD, Boeve BF, Kantarci K, Petrucelli L, Lowe VJ, Jack CR Jr., Petersen RC, Parisi JE, Dickson DW, 2017 Tau aggregation influences cognition and hippocampal atrophy in the absence of beta-amyloid: a clinico-imaging-pathological study of primary age-related tauopathy (PART). Acta Neuropathol. 133, 705–715. [PubMed: 28160067]

Joshi AD, Pontecorvo MJ, Clark CM, Carpenter AP, Jennings DL, Sadowsky CH, Adler LP, Kovnat KD, Seibyl JP, Arora A, Saha K, Burns JD, Lowrey MJ, Mintun MA, Skovronsky DM, Florbetapir FSI, 2012 Performance characteristics of amyloid PET with florbetapir F 18 in patients with alzheimer's disease and cognitively normal subjects. J. Nucl. Med 53, 378–384. [PubMed: 22331215]

Knopman DS, Jack CR Jr., Lundt ES, Wiste HJ, Weigand SD, Vemuri P, Lowe VJ, Kantarci K, Gunter JL, Senjem ML, Mielke MM, Machulda MM, Roberts RO, Boeve BF, Jones DT, Petersen RC, 2015 Role of beta-amyloidosis and neurodegeneration in subsequent imaging changes in mild cognitive impairment. JAMA Neurol. 72, 1475–1483. [PubMed: 26437123]

Kosik KS, Joachim CL, Selkoe DJ, 1986 Microtubule-associated protein tau (tau) is a major antigenic component of paired helical filaments in Alzheimer disease. Proc. Natl. Acad. Sci. U. S. A 83, 4044–4048. [PubMed: 2424016]

Landau SM, Mintun MA, Joshi AD, Koeppe RA, Petersen RC, Aisen PS, Weiner MW, Jagust WJ, Alzheimer's Disease Neuroimaging I, 2012 Amyloid deposition, hypometabolism, and longitudinal cognitive decline. Ann. Neurol 72, 578–586. [PubMed: 23109153]

Mattsson N, Insel PS, Nosheny R, Tosun D, Trojanowski JQ, Shaw LM, Jack CR Jr., Donohue MC, Weiner MW, Alzheimer's Disease Neuroimaging I, 2014 Emerging beta-amyloid pathology and accelerated cortical atrophy. JAMA Neurol. 71, 725–734. [PubMed: 24781145]

Mattsson N, Scholl M, Strandberg O, Smith R, Palmqvist S, Insel PS, Hagerstrom D, Ohlsson T, Zetterberg H, Jogi J, Blennow K, Hansson O, 2017 (18)F-AV-1451 and CSF T-tau and P-tau as biomarkers in Alzheimer's disease. EMBO Mol. Med 9, 1212–1223. [PubMed: 28743782]

Mormino EC, 2014 The relevance of beta-amyloid on markers of Alzheimer's disease in clinically normal individuals and factors that influence these associations. Neuropsychol. Rev 24, 300–312. [PubMed: 25108368]

Mormino EC, Kluth JT, Madison CM, Rabinovici GD, Baker SL, Miller BL, Koeppe RA, Mathis CA, Weiner MW, Jagust WJ, 2009 Episodic memory loss is related to hippocampal-mediated beta-amyloid deposition in elderly subjects. Brain 132, 1310–1323. [PubMed: 19042931]

Mormino EC, Sperling RA, Holmes AJ, Buckner RL, De Jager PL, Smoller JW, Sabuncu MR, Alzheimer's Disease Neuroimaging I, 2016 Polygenic risk of Alzheimer disease is associated with early- and late-life processes. Neurology 87, 481–488. [PubMed: 27385740]

Morris JC, 1993 The Clinical Dementia Rating (CDR): current version and scoring rules. Neurology 43, 2412–2414.

Morris JC, Roe CM, Grant EA, Head D, Storandt M, Goate AM, Fagan AM, Holtzman DM, Mintun MA, 2009 Pittsburgh compound B imaging and prediction of progression from cognitive normality to symptomatic Alzheimer disease. Arch. Neurol 66, 1469–1475. [PubMed: 20008650]

Morris JC, Storandt M, Miller JP, McKeel DW, Price JL, Rubin EH, Berg L, 2001 Mild cognitive impairment represents early-stage Alzheimer disease. Arch. Neurol 58, 397–405. [PubMed: 11255443]

Nosheny RL, Insel PS, Truran D, Schuff N, Jack CR Jr., Aisen PS, Shaw LM, Trojanowski JQ, Weiner MW, Alzheimer's Disease Neuroimaging I, 2015 Variables associated with hippocampal atrophy rate in normal aging and mild cognitive impairment. Neurobiol. Aging 36, 273–282. [PubMed: 25175807]

Oh H, Madison C, Villeneuve S, Markley C, Jagust WJ, 2013 Association of gray matter atrophy with age, beta-amyloid, and cognition in aging. Cereb. Cortex 24, 1609–1618. [PubMed: 23389995]

Palmqvist S, Scholl M, Strandberg O, Mattsson N, Stomrud E, Zetterberg H, Blennow K, Landau S, Jagust W, Hansson O, 2017 Earliest accumulation of beta-amyloid occurs within the default-mode network and concurrently affects brain connectivity. Nat. Commun 8, 1214. [PubMed: 29089479]

Petersen RC, Smith GE, Waring SC, Ivnik RJ, Tangalos EG, Kokmen E, 1999 Mild cognitive impairment: clinical characterization and outcome. Arch. Neurol 56, 303–308. [PubMed: 10190820]

Resnick SM, Pham DL, Kraut MA, Zonderman AB, Davatzikos C, 2003 Longitudinal magnetic resonance imaging studies of older adults: a shrinking brain. J. Neurosci 23, 3295–3301. [PubMed: 12716936]

Rowe CC, Ellis KA, Rimajova M, Bourgeat P, Pike KE, Jones G, Fripp J, Tochon-Danguy H, Morandeau L, O'Keefe G, Price R, Raniga P, Robins P, Acosta O, Lenzo N, Szoeke C, Salvado O, Head R, Martins R, Masters CL, Ames D, Villemagne VL, 2010 Amyloid imaging results from the Australian Imaging, Biomarkers and Lifestyle (AIBL) study of aging. Neurobiol. Aging 31, 1275–1283. [PubMed: 20472326]

Rowe CC, Ng S, Ackermann U, Gong SJ, Pike K, Savage G, Cowie TF, Dickinson KL, Maruff P, Darby D, Smith C, Woodward M, Merory J, Tochon-Danguy H, O'Keefe G, Klunk WE, Mathis CA, Price JC, Masters CL, Villemagne VL, 2007 Imaging beta-amyloid burden in aging and dementia. Neurology 68, 1718–1725. [PubMed: 17502554]

Schott JM, Bartlett JW, Fox NC, Barnes J, 2010 Increased brain atrophy rates in cognitively normal older adults with low cerebrospinal fluid Abeta1–42. Ann. Neurol 68, 825–834. [PubMed: 21181717]

Sowell ER, Peterson BS, Kan E, Woods RP, Yoshii J, Bansal R, Xu D, Zhu H, Thompson PM, Toga AW, 2007 Sex differences in cortical thickness mapped in 176 healthy individuals between 7 and 87 years of age. Cereb. Cortex 17, 1550–1560. [PubMed: 16945978]

Storandt M, Mintun MA, Head D, Morris JC, 2009 Cognitive decline and brain volume loss as signatures of cerebral Amyloid-beta peptide deposition identified with Pittsburgh compound B: cognitive decline associated with Abeta deposition. Arch. Neurol 66, 1476–1481. [PubMed: 20008651]

Thal DR, Rub U, Orantes M, Braak H, 2002 Phases of A beta-deposition in the human brain and its relevance for the development of AD. Neurology 58, 1791–1800. [PubMed: 12084879]

Tosun D, Schuff N, Truran-Sacrey D, Shaw LM, Trojanowski JQ, Aisen P, Peterson R, Weiner MW, 2010 Relations between brain tissue loss, CSF biomarkers, and the ApoE genetic profile: a longitudinal MRI study. Neurobiol. Aging 31, 1340–1354. [PubMed: 20570401]

Walhovd KB, Fjell AM, Reinvang I, Lundervold A, Dale AM, Eilertsen DE, Quinn BT, Salat D, Makris N, Fischl B, 2005 Effects of age on volumes of cortex, white matter and subcortical structures. Neurobiol. Aging 26, 1261–1270. [PubMed: 16005549]

Wechsler D, 1987 WMS-R Wechsler Memory Scale - Revised Manual. Harcourt Brace Jovanovich, Inc, New York.

Whitwell JL, Tosakulwong N, Weigand SD, Senjem ML, Lowe VJ, Gunter JL, Boeve BF, Knopman DS, Dickerson BC, Petersen RC, Jack CR Jr., 2013 Does amyloid deposition produce a specific atrophic signature in cognitively normal subjects? Neuroimage Clin. 2, 249–257. [PubMed: 24179779]

Whitwell JL, Wiste HJ, Weigand SD, Rocca WA, Knopman DS, Roberts RO, Boeve BF, Petersen RC, Jack CR Jr., 2012 Comparison of imaging biomarkers in the alzheimer disease neuroimaging initiative and the Mayo clinic study of aging. Arch. Neurol 69, 614–622. [PubMed: 22782510]

Wilson RS, Yu L, Trojanowski JQ, Chen EY, Boyle PA, Bennett DA, Schneider JA, 2013 TDP-43 pathology, cognitive decline, and dementia in old age. JAMA Neurol. 70, 1418–1424. [PubMed: 24080705]

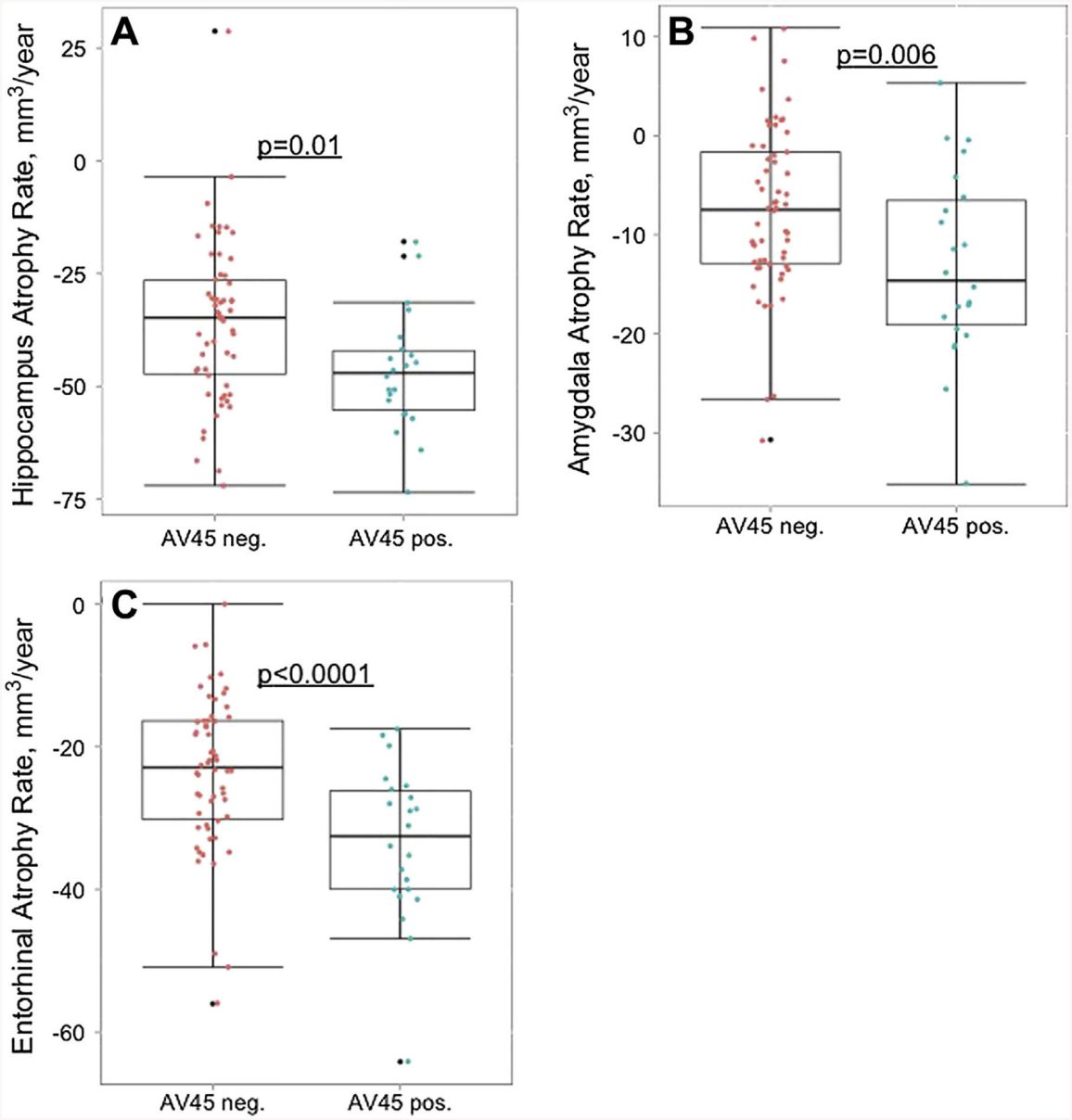

Fig. 1.

Effect of amyloid status on regional atrophy rate. Box and whisker plots showing atrophy rates in hippocampus (A), amygdala (B), and entorhinal cortex (C), 3 regions in which amyloid status is significantly associated with longitudinal atrophy rate. Top and bottom limits of the boxes represent the 25th and 75th percentile, box centerlines represent the median value, and whiskers extend to the most extreme data point which is no more than 1.5 times the length of the box away from the box. Atrophy rates of individual participants are indicated by red (Aβ−) or cyan (Aβ+) dots. In this and all subsequent figures, higher atrophy rates are indicated by lower values on the y-axis. Abbreviation: Aβ, Amyloid-β.

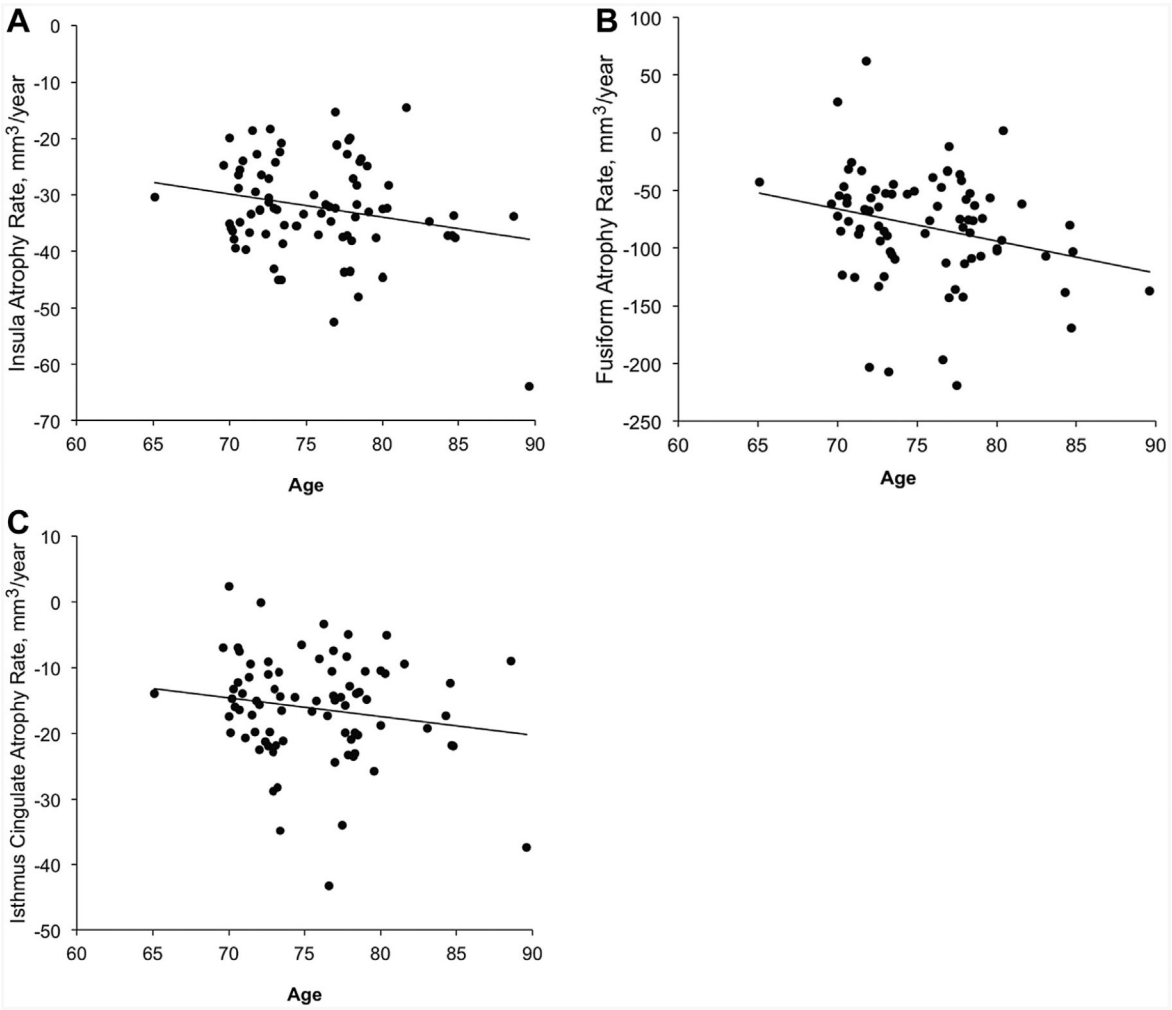

Fig. 2.

Effect of age on regional atrophy rate. Scatter plots showing the association between age and longitudinal atrophy rate in 3 regions. Multivariable linear mixed effects analysis (black lines) shows significant associations between age and atrophy rate in the insula (A, $p = 0.05$), fusiform gyrus (B, $p = 0.03$), and isthmus cingulate (C, $p = 0.05$). Atrophy rates of individual participants are indicated by black dots. Higher atrophy rates are indicated by lower values on the y-axis. Abbreviation: Aβ, Amyloid-β.

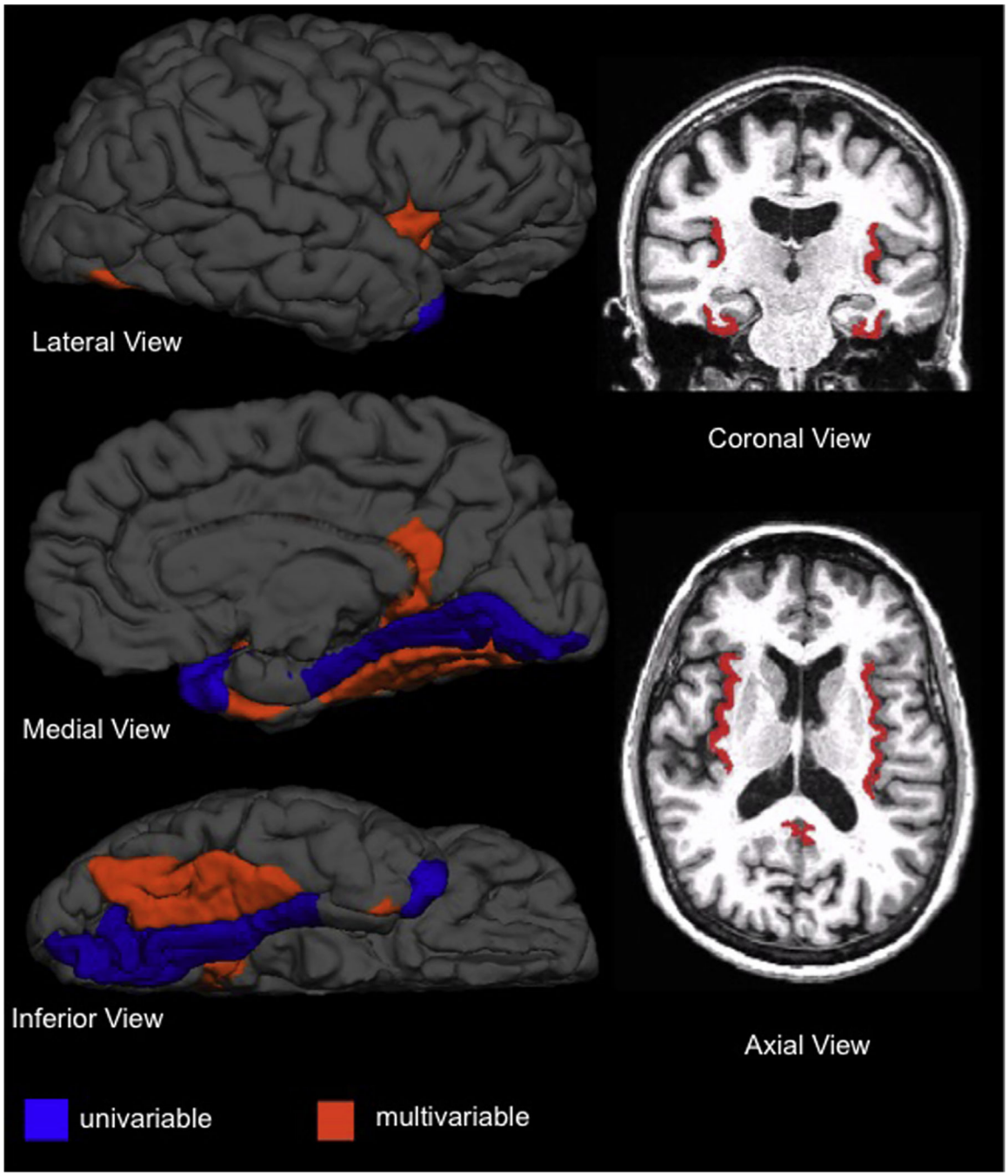

Fig. 3.

Regions with significant associations between age and atrophy rates. FreeSurfer ROIs with significant associations between age and atrophy rate are shown in red and blue. Regions with a significant association between age and atrophy rate in the univariable model, shown in blue, include the temporal pole and lingual gyrus. When accounting for Aβ status, significant associations between age and atrophy rate are present in adjacent but nonoverlapping areas within the temporal lobe and occipital lobe (red) including the insula,

fusiform gyrus, and isthmus cingulate. Abbreviations: Aβ, Amyloid-β; ROIs, regions of interest.

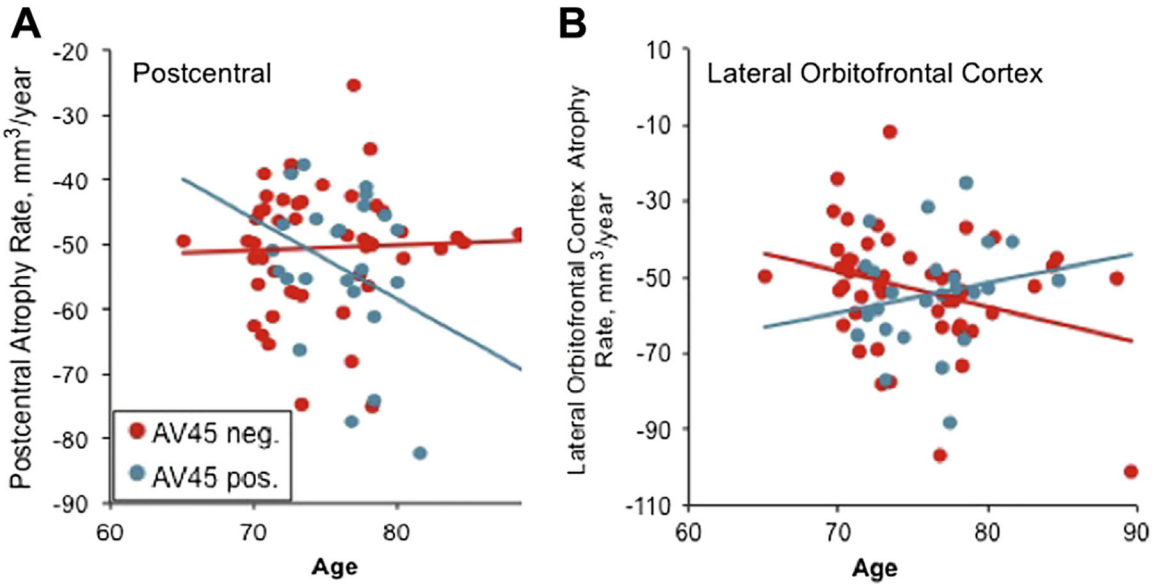

Fig. 4.

Effects of age on atrophy rates in Aβ+ and Aβ− participants. Scatter plots showing the effect of age on atrophy rate in a cohort of participants classified as Aβ− (red circles) or Aβ+ (cyan circles). Linear mixed effects models (solid red and cyan lines) show a significant interaction between age and Aβ status in 2 regions. In (A) the postcentral gyrus, agerelated atrophy rate is greater in Aβ+ than in Aβ− ($p = 0.006$), whereas in (B) the lateral orbitofrontal cortex, age-related atrophy rate is greater in Aβ− than in Aβ+ ($p = 0.05$). Higher atrophy rates are indicated by lower values on the y-axis. Abbreviation: Aβ, amyloid-β.

Table 1

Demographics of participants included in this study

	Total	Aβ+	Aβ−
Number of participants (%)	80	27 (33.8%)	53 (66.2%)
Age (mean ± SD, range)	75.6 ± 4.6, 65.1–89.6	76.1± 3.4, 71.3–84.8	75.4 ± 5.2, 65.1–89.6
Number female (%)	41 (51.3%)	14 (51.9%)	27 (51.0%)
Years of education (mean ± SD, range)	16.1 ± 3.0, 6–20	15.6 ± 3.1, 6–20	16.4 ± 2.9, 8–20
APOE ε4+ (% of total)	19 (23.8%)	11 (40.7%)	8 (15.1%)[a]
White matter lesions × 10^{-3} (mean ± SD, range)	3.9 ± 2.2, 1.2–11.1	3.8 ± 2.2, 1.2–10.0	3.9 ± 2.2, 1.2–11.0
Intracranial volume × 10^{-6} (mean ± SD, range)	1.5 ± 0.15, 1.2–1.8	1.5 ± 0.17, 1.3–1.8	1.5 ± 0.15, 1.2–1.9
Total tau (mean ± SD, range)	72.4 ± 32.2, 32–184	92.3 ± 39.6, 37–184	62.7 ± 22.9,[a] 32–120
pTau (mean ± SD, range)	24.4 ± 10.8, 12–59	31.7 ± 12.6, 15–49	20.9 ± 8.0,[a] 12–52

Key: Aβ, Amyloid-β; pTau, phosphorylated tau.

[a] $p < 0.05$ versus Aβ+.

Table 2

Regional atrophy rates from 41 FreeSurfer regions of interest in Aβ+ and Aβ− participants

	Aβ+				Aβ−			
	Region	**Rate**	**Effect size**	***p* value**	**Region**	**Rate**	**Effect size**	***p* value**
1	Hippocampus	−46.87	−2.321	0	Inferior temporal	−96.81	−1.701	0
2	Entorhinal	−38.04	−1.669	0	Lateral occipital	−76.11	−1.356	0
3	Medial orbitofrontal	−41.40	−1.404	0	Hippocampus	−30.70	−1.237	0
4	Superior frontal	−153.20	−1.366	0	Parahippocampus	−17.57	−1.216	0
5	Pars orbitalis	−22.43	−1.355	0	Fusiform	−71.05	−1.209	0
6	Superior temporal	−78.02	−1.331	0	Inferior parietal	−96.13	−1.167	0
7	Lateral orbitofrontal	−55.53	−1.296	0	Superior temporal	−75.81	−1.154	0
8	Lingual	−38.62	−1.289	0	Pars orbitalis	−14.83	−1.115	0
9	Parahippocampus	−25.78	−1.228	0	Middle temporal	−92.20	−1.101	0
10	Middle temporal	−103.79	−1.158	0	Medial orbitofrontal	−26.81	−1.077	0
11	Isthmus cingulate	−13.51	−1.089	0	Entorhinal	−19.72	−1.048	0
12	Rostral middle frontal	−92.23	−1.053	0	Caudal middle frontal	−46.69	−1.009	0
13	Temporal pole	−19.21	−1.030	0	Superior frontal	−118.93	−0.998	0
14	Pars opercularis	−27.61	−1.026	0	Supramarginal	−66.88	−0.997	0
15	Amygdala	−17.61	−0.982	0	Precentral	−93.76	−0.975	0
16	Bankssts	−17.82	−0.979	0	Isthmus cingulate	−14.71	−0.947	0
17	Insula	−30.66	−0.971	0	Insula	−24.62	−0.937	0
18	Inferior temporal	−94.47	−0.968	0	Lingual	−32.64	−0.921	0
19	Superior parietal	−94.78	−0.927	0	Rostral middle frontal	−85.22	−0.908	0
20	Posterior cingulate	−19.04	−0.897	0.0026	Superior parietal	−86.26	−0.868	0
21	Inferior parietal	−100.88	−0.886	0	Transverse temporal	−6.95	−0.861	0
22	Pars triangularis	−21.66	−0.847	0.0024	Lateral orbitofrontal	−46.43	−0.822	0
23	Precuneus	−68.78	−0.791	0.0013	Thalamus	−49.96	−0.809	0
24	Fusiform	−78.83	−0.761	0.0012	Precuneus	−51.10	−0.788	0
25	Paracentral	−19.90	−0.760	0.0104	Pars triangularis	−20.85	−0.783	0
26	Thalamus	−38.93	−0.759	0.007	Bankssts	−13.91	−0.772	0
27	Putamen	−27.70	−0.740	0.0117	Postcentral	−39.00	−0.762	0

	Aβ+				Aβ−			
	Region	**Rate**	**Effect size**	***p* value**	**Region**	**Rate**	**Effect size**	***p* value**
28	Accumbens area	−7.27	−0.701	0.0178	Pars opercularis	−24.25	−0.753	0
29	Postcentral	−53.92	−0.689	0.0091	Paracentral	−24.03	−0.749	0
30	Caudal middle frontal	−37.39	−0.685	0.0136	Cuneus	−16.39	−0.714	0
31	Cuneus	−15.40	−0.684	0.0147	Putamen	−38.65	−0.687	0
32	Frontal pole	−6.99	−0.646	0.014	Temporal pole	−14.60	−0.628	0
33	Lateral occipital	−54.11	−0.635	0.0211	Posterior cingulate	−13.94	−0.613	0
34	Rostral anterior cingulate	−11.18	−0.605	0.0201	Caudal anterior cingulate	−7.03	−0.608	0.0024
35	Supramarginal	−48.55	−0.565	0.0342	Rostral anterior cingulate	−10.23	−0.564	0.0012
36	Caudate	−27.98	−0.565	0.0219	Caudate	−20.13	−0.472	0.0164
37	Caudal anterior cingulate	−8.96	−0.564	0.0305	Frontal pole	−3.02	−0.449	0.0588
38	Transverse temporal	−4.69	−0.544	0.0533	Accumbens area	−7.80	−0.389	0
39	Precentral	−52.41	−0.389	0.1406	Amygdala	−5.23	−0.335	0.0688
40	Pericalcarine	−1.81	−0.134	0.6858	Pericalcarine	−6.74	−0.329	0.0812
41	Pallidum	5.04	0.274	0.2517	Pallidum	−0.45	−0.022	0.9043

Regions are listed in order of the effect size for each subgroup (Aβ+ and Aβ−).

Key: Aβ, Amyloid-β.